Design of a Device to Assist Sit-To-Stand Motion for Humans

A THESIS

submitted by

Vyankatesh Raghav Ashtekar

in partial fulfillment of the requirements for the award of the degree of

MASTER OF TECHNOLOGY
in
MECHANICAL DESIGN

DEPARTMENT OF MECHANICAL ENGINEERING
INDIAN INSTITUTE OF TECHNOLOGY MADRAS
CHENNAI 600036

May 2017

Department of Mechanical Engineering

Indian Institute of Technology Madras

Certificate

This is to certify that the project titled **"Design of a Device to Assist Sit-To-Stand Motion for Humans"**, submitted by **"Vyankatesh Raghav Ashtekar (ME15M090)"**,to the Indian Institute of Technology, Madras, in partial fulfillment of the requirements for the award of the degree of ***Master of Technology in Mechanical Design Engineering***, is a bona-fide record of project work carried out by him in *Department of Mechanical Engineering, I.I.T. Madras.* The contents of this project in full or in parts have not been submitted to any other institution for an award of any degree or diploma.

Dr. Sourav Rakshit
Project Guide,
Machine Design Section,
Department of Mechanical Engineering,
Indian Institute of Technology, Madras,
Chennai, Tamil Nadu-600036.

Dr.B.V.S.S.S. Prasad
Professor & Head of the Department,
Department of Mechanical Engineering,
Indian Institute of Technology, Madras,
Chennai, Tamil Nadu -600036.

Date:
Place:

Acknowledgments

I express my sincere gratitude and thanks to Prof. Sourav Rakshit for providing me the opportunity to work with him during my graduate study. His guidance and continuous encouragement for innovation were crucial for me to accomplish the project objectives. He opened all doors possible facilitating practical implementation of the project. I thank him for helping me promptly in resolving my scientific queries. Lastly, thank you sir, for believing in me as I progressed.

I would like to thank the entire faculty at Machine Design Section, Department of Mechanical Engineering who helped me complete my graduate course work smoothly. Knowledge of the courses ED5260 and ED5314 conducted by Prof. Sandipan Bandyopadhyay at Department of Engineering Design went along way in inculcating the concepts of kinematics and dynamics of rigid bodies. I also thank Prof. Sujatha Srinivasan for allowing me to use equipment at TTK center for Rehabilitation Research and Device Developement for the sit-to-stand experiments.

I thank the Head of workshop, Machine Design Section Mr. Vijaykumar and Mr. Murali for helping out in manufacturing the device prototype. I thank my friends for their continuous support during my stay at IIT Madras. Finally, I am short of words while I express sentiments about my parents for their sacrifices to get me where I stand in this world today.

Abstract

KEYWORDS: Sit-to-stand, Lagrangian dynamics, Recursive Newton-Euler equations, Motion prediction, Dynamic effort, B-spline

This project aims to conceptualize and design a device to assist Sit-to-Stand (STS) motion for humans. Kinematics and dynamics of unaided STS motion for a simplified model of human with arms folded and close to chest, in sagittal plane is studied for the device design. The formulation is extended for analyzing aided STS motion. Dynamics of closed loop mechanisms or constrained dynamic systems is studied in five different ways. Imitation of natural STS trajectory for aforementioned human model is accomplished by optimal control with an unknown trajectory parametrized in terms of a cubic B-spline. Human performance measure optimized during natural STS motion is defined suitably and numerical optimization is carried out to obtain said trajectory.

Human is modeled as a 3$\underline{\mathrm{R}}$ planar linkage moving between specified initial position of sitting to final position of standing. Inverse dynamics for unconstrained systems is a straight forward substitution problem. Human performance measure to be minimized over the path is defined as dynamic effort. Dynamic effort is defined as square of norm of joint generalized force vector. The optimization is carried out using other conditions of optimality such as total work done over the path too. Only dynamic effort of all the optimality measures tried out, leads to humanly trajectories. Predicted trajectories are compared to the captured experimental ones to ascertain their validity.

For simulation of aided STS motion, amongst a variety of possible support strategies, one with the minimalistic approach is chosen. Human along with the device is modeled as a single loop six bar planar mechanism with five revolute joints and one prismatic joint. Mobility of the mechanism turns out to be three. Knee, hip and the prismatic joint are considered as the active degrees of freedom while ankle, shoulder and interface of the device with ground remain passive degrees of freedom. Two different joint spaces are chosen for simulations - first is a set of variables defined by DH convention and second set is defined with space fixed variables.

Equations of motion for the closed loop mechanism are derived adopting recursive Newton Euler equations using body fixed coordinates. Derivation of the same using Lagrangian approach with space fixed coordinates is also accomplished. Both the formulations are verified with each other in closed form. The Newton-Euler formulation facilitates calculation of joint reaction forces which are needed during constrained optimization as well as validation of the trajectories.

Results reveal that the simulated joint torques in case of aided STS motion are never larger than that of natural STS motion. This signifies that the device may not add to efforts in natural movement. Further, it is observed from the simulations that the torque delivered by knee is reduce greatly while using aid of the device. Experimental data of ground reaction forces suggest usefulness of the device too.

Contents

List of Figures

List of Tables

Abbreviations

STS	Sit-to-Stand
DH	Denavit-Hartenberg
OL	Open loop
CL	Closed loop
GRF	Ground reaction force
ZMP	Zero moment point

Chapter 1

Introduction

Motivation

Sit-to-stand (STS) is a common activity performed repeatedly in daily lives which requires relatively high joint torques and a full-bodied coordination of lower and upper extremities with postural stability [13]. STS may be defined as one of the key determinants of functional independence in daily lives. Standing up is a prerequisite to majority routine movements thus mobility of those who cannot achieve it independently is crippled greatly. A person infirm to perform sit to stand movement depends on help of a second person or a good enough support. These people tend to restrict their movement in absence of a helper.

A device helping infirm to stand up will alleviate their pain allowing them to follow regular activities smoothly. A market survey (performed during the course of this project) of such sit to stand aids in India leads us to the fact that there exist very few STS movement solutions. There are quite a few stand up aids in developed nations (detailed survey is done in [14]), however the number of such solutions is quite less as compared to walking aids. Most of STS assistive devices are electrically powered. The size and weight of the electric actuators along with their batteries make the devices heavy and limits their transportability. This project aims at developing a portable STS motion aid. Both active (electrically powered) as well as passive (regenerative) devices are thought of while brainstorming for the device design. Design procedure for bio-mechanical assistive devices or rehabilitation equipment often demands practical experiments to estimate performance parameters of the device.

Planing and executing STS experiments is time and resource consuming. Motion capture system synchronized with force plates are required to generate complete dynamic model of the movement. Conducting STS experiments has many downsides. As the task is mechanically demanding, only limited repetitions of STS movement can be carried out at a time before a healthy subject loses his/her strength and starts changing the STS trajectory unknowingly. On the other hand, testing a device prototype on the injured or elderly people in order to obtain their feedback on the performance of the device may lead to new injuries to them which may affect the quality of rest of their life. Also, a lot of experiments would be required to test the device on all possible types of lower limb injuries and combination of them.

This is where computational modeling of human movements on computer platform becomes crucial. Firstly, simulation of unaided sit to stand motion is done. It is followed by more complicated simulation of human interaction with the assitive device. The benefits of computational modeling are numerous. Unlimited number of virtual experiments with different human body parameters can be carried out. Injuries can be modeled as constraints on certain force or torques. Multiple injuries can be simulated together. All of this without annoying the patients and risking their well being.

Objectives and Scope

The project objectives are twofold −

1. To study the dynamics of sit to stand motion using a computational model
   (a) Unaided STS motion in sagittal plane will be simulated
   (b) Aided STS motion in sagittal place will be simulated
2. To develop a device assisting STS movement.

1.1 Overview of Thesis

Chapter 2 reviews the concepts of rigid body dynamics used in STS trajectory prediction. Kinematics of multi-link mechanisms is discussed in section 2.1 followed by dynamics in section 2.2. Inverse dynamics formulations for open and closed loop mechanisms are discussed in sections 2.2.1 and 2.2.2 respectively.

Chapter 3 includes the computational modeling of unaided STS motion with hands folded close to chest. The simulation results are compared to those of experiments in order to test the motion prediction algorithm. Chapter 4 extends the algorithm for closed loop model of human with assistive device. The design and working of STS aid device is explained in chapter 5.

1.2 Literature Survey

The literature surveyed is classified in two categories- patent and literature survey of existing STS motion assist devices and second is the survey of past studies in motion prediction methods.

A detailed survey of devices available for assisting STS motion is included in [14]. Conventional design procedures for assistive devices rely heavily on experimental results. With motion capture technology supplying the joint angle trajectories as function of time, joint torques/ forces are calculated using inverse dynamics equations. Few such studies are surveyed for verification of computational work. The results of free STS motion have been verified with experimental joint trajectories of [7].

The trajectory optimization approach followed in this study resembles to that of [16]. The measure of effort of human during STS motion is adopted from the same work. Optimization based motion prediction is applied to a simple 2R planar robot to generate trajectories with minimal work done over the path in [16].The work published in [6] has several illustrations of OL mechanism trajectory planning with minimum joint torques and an example of closed loop motion planning. Three dimension STS motion prediction problem is undertaken and solved in [13]. A two step method for joint torques and GRF calculations using concept of ZMP is proposed in the same.

A simple and computationally efficient approach for dynamics of closed loop mechanisms using Newton-Euler formulation is discussed in [11]. The same is adopted in the computations of the study. Other approaches from [12] and [1] are also tried out during formulation of the problem.

The critical step in trajectory prediction is the optimization of dynamic effort calculated on the path of motion. The objective function is highly nonlinear and calculating analytical gradients of such function is computationally unreasonably expensive due to non-linearity of the objective function. Numerical gradients may become ill conditioned adversely influencing the optimization process. For the same reason, [6] has developed recursive calculations for analytical gradient needed in the optimization algorithm for such problems.

Chapter 2

Basic Concepts

2.1 Kinematics of Multi-Link Mechanisms

The study of kinematics is divided into two main categories −

- Forward kinematics
- Inverse kinematics

Forward kinematics is the calculation of kinematic quantities such as but not limited to position, velocity and acceleration of a certain point $\boldsymbol{P}$ on mechanism given information of position, velocity and acceleration of the joint variables $\boldsymbol{q}$. E.g.

$$\begin{aligned} \boldsymbol{P} &= f_1(\boldsymbol{q}) \\ \dot{\boldsymbol{P}} &= f_2(\boldsymbol{q}, \dot{\boldsymbol{q}}) \\ \ddot{\boldsymbol{P}} &= f_3(\boldsymbol{q}, \dot{\boldsymbol{q}}, \ddot{\boldsymbol{q}}) \end{aligned} \tag{2.1}$$

It is important to note that $\boldsymbol{q} = \boldsymbol{q}(t)$ but $\boldsymbol{P}$ is not an explicit function of time in context of the formulations discussed ahead in this report. On the other hand, calculation of joint variables $\boldsymbol{q}$ given the position of certain point $\boldsymbol{P}$ or end effector constitutes the inverse kinematics. E.g.

$$\begin{aligned} \boldsymbol{q} &= f_1^{-1}(\boldsymbol{P}) \\ \dot{\boldsymbol{q}} &= f_2^{-1}(\boldsymbol{P}, \dot{\boldsymbol{P}}) \\ \ddot{\boldsymbol{q}} &= f_3^{-1}(\boldsymbol{P}, \dot{\boldsymbol{P}}, \ddot{\boldsymbol{P}}) \end{aligned} \tag{2.2}$$

Forward kinematics of open loop mechanisms is straight forward and has unique solution. The inverse kinematics of open loop mechanism often has multiple branches of solution. In the case of forward kinematics of closed loop mechanisms, the solution has multiple branches complicating the process than that of the open loop mechanisms. On the other hand, inverse kinematic problem for closed loop mechanisms is generally easier, or of same complexity as that of open loop mechanisms.

2.1.1 The DH Convention

In order to define the coordinate transformations between frames attached to all the links of a mechanism, an unified approach based on screw theory known as DH parameters was proposed in [5]. We will be using modified DH parameters as defined in [3] throughout this study.

2.1.2 Kinematics of Closed Loop Linkages

A closed loop mechanism can have active joints only equal to the degrees of freedom of the mechanism. We will not consider the case of redundant actuations here. So, given set of joint variables $\boldsymbol{q}$, it consists of active variables $\boldsymbol{\theta}$ and passive variables $\boldsymbol{\phi}$. Hence joint space $\boldsymbol{q} = (\boldsymbol{\theta}^T, \boldsymbol{\phi}^T)^T$. To solve for the passive variables, we write suitable loop closure equation(s)

$$\boldsymbol{\eta}(\boldsymbol{q}) = \boldsymbol{\eta}(\boldsymbol{\theta}, \boldsymbol{\phi}) \tag{2.3}$$

The zeroth order forward kinematics problem for closed loop mechanisms refers to finding the solutions $\boldsymbol{\phi} = \boldsymbol{\phi}(\boldsymbol{\theta})$ to equations (2.3). The solution is found out by repeated trigonometric elimination. The first order forward kinematics solution or the joint rates of passive angles are calculated by differentiating equation (2.3) with respect to time as follows

$$\frac{\partial \boldsymbol{\eta}}{\partial \boldsymbol{\theta}} \dot{\boldsymbol{\theta}} + \frac{\partial \boldsymbol{\eta}}{\partial \boldsymbol{\phi}} \dot{\boldsymbol{\phi}} = 0 \tag{2.4}$$

$$\Rightarrow \dot{\boldsymbol{\phi}} = -\frac{\partial \boldsymbol{\eta}}{\partial \boldsymbol{\phi}}^{-1} \frac{\partial \boldsymbol{\eta}}{\partial \boldsymbol{\theta}} \dot{\boldsymbol{\theta}} \tag{2.5}$$

Writing $\boldsymbol{J}_{\boldsymbol{\eta\theta}} = \frac{\partial \boldsymbol{\eta}}{\partial \boldsymbol{\theta}}$, $\boldsymbol{J}_{\boldsymbol{\eta\phi}} = \frac{\partial \boldsymbol{\eta}}{\partial \boldsymbol{\phi}}$ we obtain -

$$\dot{\boldsymbol{\phi}} = \boldsymbol{J}_{\boldsymbol{\phi\theta}} \dot{\boldsymbol{\theta}} \tag{2.6}$$

With $\boldsymbol{J}_{\boldsymbol{\phi\theta}} = -\boldsymbol{J}_{\boldsymbol{\eta\phi}}^{-1} \boldsymbol{J}_{\boldsymbol{\phi\theta}}$, and $\det\big(\boldsymbol{J}_{\boldsymbol{\eta\phi}}\big) \neq 0$. Similarly $\ddot{\boldsymbol{\phi}}$ can be calculated in terms of $\boldsymbol{\theta}$, $\dot{\boldsymbol{\theta}}$, and $\ddot{\boldsymbol{\theta}}$ by differentiating equation (2.6).

2.1.3 Singularities

Before we move to dynamics, it is important to get insight into the conditions which when occured rescind the calculations of dynamics. Singularities in the case of closed loop mechanisms can be classified into two types- Type-I and Type-II.

Type I singularity is encountered while solving the inverse kinematics of open loop or closed loop mechanisms. The singularity occurs at the place where branches of inverse kinematics meet. This type of singularity results in loosing one or more degrees of freedom of the mechanism.

Type II singularity is encountered while solving the forward kinematics of closed loop mechanisms. The singularity occurs at the place where branches of forward kinematics meet. This type of singularity results in gain of degrees of freedom of the mechanism.

2.2 Multi-Body Dynamics

The report will discuss methods of inverse dynamics only. Inverse dynamics involves calculation of generalized forces given joint variables, their first and second derivatives. We calculate joint variables and their derivatives by performing inverse kinematics on given trajectory of a certain point on mechanism. While dealing with closed loop mechanisms we need to exercise caution at occurrence of Type II singularities.

2.2.1 Unconstrained Systems

All the generalized coordinates assumed are independent in unconstrained systems. The number of generalized coordinates equal the degrees of freedom of mechanism. Lagrangian and recursive Newton-Euler formulations for open loop systems are discussed ahead.

Lagrangian Approach

The Lagrangian is defined as

$$L(\boldsymbol{q}, \dot{\boldsymbol{q}}) = T(\boldsymbol{q}, \dot{\boldsymbol{q}}) - V(\boldsymbol{q}) \tag{2.7}$$

where T is kinetic energy and V is potential energy associated with conservative forces [8]. Using Hamiltonian principle, equations of motion can be derived by obtaining the stationary value of action integral I.

$$I = \int_{t_1}^{t_2} L(\boldsymbol{q}, \dot{\boldsymbol{q}}) \mathrm{d}t \tag{2.8}$$

$$\delta I = 0 \tag{2.9}$$

Equation (2.9) after manipulations (which use the fact that all the generalized coordinates are independent), gives

$$\frac{d}{dt}\Big(\frac{\partial L}{\partial \dot{\boldsymbol{q}}}\Big) - \frac{\partial L}{\partial \boldsymbol{q}} = 0 \tag{2.10}$$

Above derivation with a few more manipulations and D'Alembert's principle for dynamic equilibrium gives

$$\frac{d}{dt}\Big(\frac{\partial L}{\partial \dot{\boldsymbol{q}}}\Big) - \frac{\partial L}{\partial \boldsymbol{q}} = \boldsymbol{\tau} \tag{2.11}$$

Where $\boldsymbol{\tau}$ are externally applied generalized forces. Above equation can be written in matrix form as

$$\boldsymbol{M}(\boldsymbol{q})\ddot{\boldsymbol{q}} + \boldsymbol{C}(\boldsymbol{q}, \dot{\boldsymbol{q}})\dot{\boldsymbol{q}} + \boldsymbol{G} = \boldsymbol{\tau} \tag{2.12}$$

The mass matrix $\boldsymbol{M}$ contains all the inertia terms. The $\boldsymbol{C}$ matrix contains centripetal and Coriolis force terms and the $\boldsymbol{G}$ matrix contains all the forces due to gravity. Note that $\boldsymbol{C}$ matrix can be derived from $\boldsymbol{M}$ matrix alone as given in [10]. The inverse dynamics of open loop mechanisms is a straight forward substitution problem. We get generalized forces by substituting joint variables and their derivatives in the equations of motion (2.12). Lagrangian approach leading to the $\boldsymbol{M}$, $\boldsymbol{C}$, $\boldsymbol{G}$ matrices gives us insight into the characteristics of the mechanism. However, te approach is computationally expensive for real time computation.

Newton-Euler Approach

In this section we will discuss $\mathcal{O}(\mathcal{N})$ recursive inverse dynamics of open loop mechanisms using Newton-Euler formulation. Newton's law and Euler's equation for each link $\{i\}$

$$\begin{aligned} {}^{0}\boldsymbol{F} &= m_i \, {}^{0}\dot{\boldsymbol{V}}_{C_i} \\ {}^{0}\boldsymbol{N} &= {}^{C_i}[I_i] \, {}^{0}\dot{\boldsymbol{\omega}}_i + {}^{0}\boldsymbol{\omega} \times {}^{C_i}[I_i] \, {}^{0}\boldsymbol{\omega}_i \end{aligned} \tag{2.13}$$

Where m_i, C_i and $[I_i]$ are the mass, center of mass and inertia of link $\{i\}$. The pre-superscript indicates the frame in which the quantities are calculated, 0 being the ground frame.

Outward Recursion $\quad \mathbf{i : 0 \rightarrow N - 1}$

$$\begin{aligned} R\text{:}\ {}^{i+1}\boldsymbol{\omega}_{i+1} &= {}^{i+1}_{i}[R] \, {}^{i}\boldsymbol{\omega}_i + \dot{\theta}_{i+1} \, {}^{i+1}\boldsymbol{z}_{i+1} \\ P\text{:}\ {}^{i+1}\boldsymbol{\omega}_{i+1} &= {}^{i+1}_{i}[R] \, {}^{i}\boldsymbol{\omega}_i \end{aligned} \tag{2.14}$$

$$\begin{aligned} R\text{:}\ {}^{i+1}\dot{\boldsymbol{\omega}}_{i+1} &= {}^{i+1}_{i}[R] \, {}^{i}\dot{\boldsymbol{\omega}}_i + {}^{i+1}_{i}[R] \, {}^{i}\boldsymbol{\omega}_i \times \dot{\theta}_{i+1} \, {}^{i}\boldsymbol{z} + \ddot{\theta}_{i+1} \, {}^{i+1}\boldsymbol{z}_{i+1} \\ P\text{:}\ {}^{i+1}\dot{\boldsymbol{\omega}}_{i+1} &= {}^{i+1}_{i}[R] \, {}^{i}\dot{\boldsymbol{\omega}}_i \end{aligned} \tag{2.15}$$

$$\begin{aligned} R\text{:}\ {}^{i+1}\dot{\boldsymbol{V}}_{i+1} &= {}^{i+1}_{i}[R]({}^{i}\dot{\boldsymbol{\omega}}_i \times {}^{i}\boldsymbol{p}_{i+1} + {}^{i}\boldsymbol{\omega}_i \times ({}^{i}\boldsymbol{\omega}_i \times {}^{i}\boldsymbol{p}_{i+1})) \\ P\text{:}\ {}^{i+1}\dot{\boldsymbol{V}}_{i+1} &= {}^{i+1}_{i}[R]({}^{i}\dot{\boldsymbol{\omega}}_i \times {}^{i}\boldsymbol{p}_{i+1} + {}^{i}\boldsymbol{\omega}_i \times ({}^{i}\boldsymbol{\omega}_i \times {}^{i}\boldsymbol{p}_{i+1})) + 2({}^{i+1}\boldsymbol{\omega}_{i+1} \times \dot{d}_{i+1} \, {}^{i+1}\boldsymbol{z}_{i+1}) \\ &\quad + \ddot{d}_{i+1} \, {}^{i+1}\boldsymbol{z}_{i+1} \end{aligned} \tag{2.16}$$

$$ {}^{i+1}\dot{\boldsymbol{V}}_{C_{i+1}} = {}^{i+1}\dot{\boldsymbol{V}}_{i+1} + {}^{i+1}\dot{\boldsymbol{\omega}}_{i+1} \times {}^{i+1}\boldsymbol{p}_{C_{i+1}} + {}^{i+1}\boldsymbol{\omega}_{i+1} \times ({}^{i+1}\boldsymbol{\omega}_{i+1} \times {}^{i+1}\boldsymbol{p}_{C_{i+1}}) \tag{2.17}$$

Where $\boldsymbol{\omega}_i$ is angular velocity of link$\{i\}$, $\dot{\boldsymbol{V}}$ is acceleration of body fixed frame and $\dot{\boldsymbol{V}}_{C_i}$ is acceleration of centre of mass of link $\{i\}$. The first equation in every sub-equation is for revolute joint R while the second one to be used for prismatic joint P. Joints with more degrees of freedom can be constructed as multiple sdof joints combined together. Transforming equations (2.13) to $\{i+1\}$ frame we get,

$$
\begin{aligned}
{}^{i+1}\boldsymbol{F}_{i+1} &= m_{i+1}\,{}^{i+1}\dot{\boldsymbol{V}}_{C_{i+1}} && (2.18)\\
{}^{i+1}\boldsymbol{N}_{i+1} &= {}^{C_{i+1}}[I_{i+1}]\,{}^{i+1}\dot{\boldsymbol{\omega}}_{i+1} + {}^{i+1}\boldsymbol{\omega}_{i+1} \times {}^{C_{i+1}}[I_{i+1}]\,{}^{i+1}\boldsymbol{\omega}_{i+1} && (2.19)
\end{aligned}
$$

Inward Recursion $\quad \mathbf{i} : \mathbf{N} \rightarrow \mathbf{1}$

$$
\begin{aligned}
{}^{i}\boldsymbol{f}_i &= {}_{i+1}^{i}[R]\,{}^{i+1}\boldsymbol{f}_{i+1} + {}^{i}\boldsymbol{F}_i && (2.20)\\
{}^{i}\boldsymbol{n}_i &= {}_{i+1}^{i}[R]\,{}^{i+1}\boldsymbol{n}_{i+1} + {}^{i}\boldsymbol{p}_{i+1} \times {}_{i+1}^{i}[R]\,{}^{i+1}\boldsymbol{f}_{i+1} + {}^{i}\boldsymbol{p}_{C_i} \times {}^{i}\boldsymbol{F}_i + {}^{i}\boldsymbol{N}_i && (2.21)\\
R: \quad \boldsymbol{\tau}_i &= {}^{i}\boldsymbol{n}_i \cdot {}^{i}\boldsymbol{z}_i \\
P: \quad \mathcal{F}_i &= {}^{i}\boldsymbol{f}_i \cdot {}^{i}\boldsymbol{z}_i && (2.22)
\end{aligned}
$$

Where $\boldsymbol{\tau_i}$ and $\mathcal{F}_\rangle$ are the actuator torque or force at joint $\{i\}$. As each joint is considered to be single degree of freedom joint, number of actuated joints equals to the number of degrees of freedom equals to the number of equations of motion.

2.2.2 Constrained Systems

Lagrangian Approach

Equations of motion for closed loop mechanism in matrix form can be written as:

$$\boldsymbol{M}(\boldsymbol{q})\ddot{\boldsymbol{q}} + \boldsymbol{C}(\boldsymbol{q}, \dot{\boldsymbol{q}})\dot{\boldsymbol{q}} + \boldsymbol{G} = \boldsymbol{\tau} + \boldsymbol{\tau}^c \tag{2.23}$$

Where $\boldsymbol{M}(\boldsymbol{q})$ is mass matrix, $\boldsymbol{C}(\boldsymbol{q}, \dot{\boldsymbol{q}})\dot{\boldsymbol{q}}$ contains the centripetal and coriolis terms and $\boldsymbol{G}$ contains forces due to gravity. On the right hand side, the vectors $\boldsymbol{\tau}, \boldsymbol{\tau}^c$ represent applied generalized fores and the forces arising out of the kinematic constraints respectively. The constraint force $\boldsymbol{\tau}^c$ can be written as $\boldsymbol{J}_{\boldsymbol{\eta q}}^T \boldsymbol{\lambda}$ [10]. Where

$$\boldsymbol{J}_{\boldsymbol{\eta q}} = \frac{\partial \boldsymbol{\eta}}{\partial \boldsymbol{q}} \tag{2.24}$$

Equation (2.23) can be written as

$$\boldsymbol{M}(\boldsymbol{q})\ddot{\boldsymbol{q}} + \boldsymbol{C}(\boldsymbol{q}, \dot{\boldsymbol{q}})\dot{\boldsymbol{q}} + \boldsymbol{G} = \boldsymbol{\tau} + \boldsymbol{J}_{\boldsymbol{\eta q}}^{T}\boldsymbol{\lambda} \tag{2.25}$$

Where $\boldsymbol{\lambda}$ is a vector of Lagrange multipliers. $\boldsymbol{\lambda}$ can be eliminated in various ways.

Active Joint Space formulation

Here we follow the approach of complete elimination of passive joint variables. Consider the mapping of active joint rates $\dot{\boldsymbol{\theta}}$ into the rate of configuration space variable $\dot{\boldsymbol{q}}$

$$\dot{\boldsymbol{q}} = \boldsymbol{J}_{\boldsymbol{q\theta}}\dot{\boldsymbol{\theta}} \tag{2.26}$$

$$\text{where } \boldsymbol{J}_{\boldsymbol{q\theta}} = \begin{pmatrix} \boldsymbol{I}_3 \\ \boldsymbol{J}_{\boldsymbol{\theta\phi}} \end{pmatrix} \tag{2.27}$$

Differentiating equation (2.26) and substituting it in (2.25) and pre-multiplying with ${\boldsymbol{J}_{\boldsymbol{q\theta}}}^{T}$ we get:

$$\boldsymbol{J}_{\boldsymbol{q\theta}}^{\boldsymbol{T}}\boldsymbol{M}\boldsymbol{J}_{\boldsymbol{q\theta}}\ddot{\boldsymbol{\theta}} + {\boldsymbol{J}_{\boldsymbol{q\theta}}}^{T}\big(\boldsymbol{M}\dot{\boldsymbol{J}_{\boldsymbol{q\theta}}} + \boldsymbol{C}\boldsymbol{J}_{\boldsymbol{q\theta}}\big)\dot{\boldsymbol{\theta}} + {\boldsymbol{J}_{\boldsymbol{q\theta}}}^{T}\boldsymbol{G} = {\boldsymbol{J}_{\boldsymbol{q\theta}}}^{T}\boldsymbol{\tau} + {\boldsymbol{J}_{\boldsymbol{q\theta}}}^{T}{\boldsymbol{J}_{\boldsymbol{\eta q}}}^{T}\boldsymbol{\lambda} \tag{2.28}$$

It is interesting to note that

$$\begin{aligned} &\boldsymbol{\eta}(\boldsymbol{q}) = 0 \\ \Rightarrow\ &\boldsymbol{J}_{\boldsymbol{\eta q}}\dot{\boldsymbol{q}} = 0 \\ \Rightarrow\ &(\boldsymbol{J}_{\boldsymbol{\eta q}}\boldsymbol{J}_{\boldsymbol{q\theta}})\dot{\boldsymbol{\theta}} = 0 \end{aligned} \tag{2.29}$$

For arbitrary input joint rate $\dot{\boldsymbol{\theta}}$, $\boldsymbol{J}_{\boldsymbol{\eta q}}\boldsymbol{J}_{\boldsymbol{q\theta}}$ should vanish. And hence $(\boldsymbol{J}_{\boldsymbol{\eta q}}\boldsymbol{J}_{\boldsymbol{q\theta}})^{T}\boldsymbol{\lambda}$ should also vanish for finite $\boldsymbol{\lambda}$. Finally equation (2.28) can be written as-

$$\boldsymbol{M}_{\boldsymbol{\theta}}\ddot{\boldsymbol{\theta}} + \boldsymbol{C}_{\boldsymbol{\theta}}\dot{\boldsymbol{\theta}} + \boldsymbol{G}_{\boldsymbol{\theta}} = \boldsymbol{\tau}_{\boldsymbol{\theta}} \tag{2.30}$$

Where $\boldsymbol{M}_{\boldsymbol{\theta}} = \boldsymbol{J}_{\boldsymbol{q\theta}}^{\boldsymbol{T}}\boldsymbol{M}\boldsymbol{J}_{\boldsymbol{q\theta}}$, $\boldsymbol{C}_{\boldsymbol{\theta}} = {\boldsymbol{J}_{\boldsymbol{q\theta}}}^{T}\big(\boldsymbol{M}\dot{\boldsymbol{J}_{\boldsymbol{q\theta}}} + \boldsymbol{C}\boldsymbol{J}_{\boldsymbol{q\theta}}\big)$ and $\boldsymbol{G}_{\boldsymbol{\theta}} = {\boldsymbol{J}_{\boldsymbol{q\theta}}}^{T}\boldsymbol{G}$ and $\boldsymbol{\tau}_{\boldsymbol{\theta}}$ is the active joint force/ torque vector. It should be noted that equation (2.30) is valid only when $\det(\boldsymbol{J}_{\boldsymbol{\theta\phi}}) \neq 0$. We use $\boldsymbol{\tau}_{\boldsymbol{\theta}}$ instead of $\boldsymbol{\tau}$ in equation (3.1) to evaluate the dynamic effort. MOre details about this formulation are given in [12]

Complete Joint Space formulations

When solving inverse dynamics, equations (2.23) can be viewed as a system of linear equations in variables $\boldsymbol{X} = \{\boldsymbol{\tau}^T, \boldsymbol{\lambda}^T\}^T$. Equations (2.23) now can be written as

$$\boldsymbol{A}\,\boldsymbol{X} = \boldsymbol{B} \tag{2.31}$$

Where,

$$\boldsymbol{A} = \begin{bmatrix} \boldsymbol{I}_{na\times na} & \boldsymbol{J}_{\boldsymbol{\eta\theta}} \\ \boldsymbol{O}_{np\times na} & \boldsymbol{J}_{\boldsymbol{\eta\phi}} \end{bmatrix} \tag{2.32}$$

$$\boldsymbol{X} = \begin{pmatrix} \boldsymbol{\tau} \\ \boldsymbol{\lambda} \end{pmatrix} \tag{2.33}$$

$$\boldsymbol{B} = \boldsymbol{M}(\boldsymbol{q})\ddot{\boldsymbol{q}} + \boldsymbol{C}(\boldsymbol{q}, \dot{\boldsymbol{q}})\dot{\boldsymbol{q}} + \boldsymbol{G} \tag{2.34}$$

Where na is number of actuated joint variables and np is number of passive joint variables. The matrix $\boldsymbol{A}$ is singular when $\boldsymbol{J}_{\boldsymbol{\eta\phi}}$ is singular. Hence, both the formulations discussed above for constrained systems are susceptible to Type II singularity. The method discussed above is used to calculate inverse dynamics in all the codes written during this project. Another new method with complete joint space is given in [1] which is insusceptible to Type II singularity.

Newton-Euler Approach

The method discussed in section (2.2.1) can be easily adapted for inverse dynamics of closed loop mechanism. One should note that the Lagrange multipliers $\boldsymbol{\lambda}$ have units of force. They are nothing but the constraint forces. A reaction force appears corresponding each kinematic constraint. The method will be explained with the help of an example of dynamics of four bar mechanism. The mechanism is cut open at one of the passive joints and the corresponding constraint forces λ_x and λ_y are acted at the tip of the mechanism. The torque of the open loop mechanism (or tree structure, if intermediate joint is cut open) thus generated is calculated taking all the joints as actuated joints using recursive equations established in section 2.2.1. But we know that all joints are not actuated. So we equate the torques of passive (green colored) joints to zero and thus solve for λ_x and λ_y. The method can be extended for multi-loop mechanism. Another elegant method is suggested in [11]. Earlier, in same section $\boldsymbol{J}_{\boldsymbol{q\theta}}$

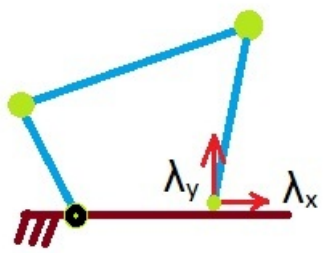

Figure 2.1: Four bar mechanism cut open at one joint

is defined as mapping of joint rates of active joints to the complete joint space. It is proven in [11] that

$$\boldsymbol{\tau} = \boldsymbol{J_{q\theta}}^T \, \boldsymbol{\tau}_o \tag{2.35}$$

Where, $\boldsymbol{\tau}$ is the required closed loop torque and $\boldsymbol{\tau_o}$ is the torque of the corresponding tree structure which can be calculated by equations in section 2.2.1

2.3 Interpolation and Approximation of Data Set

Interpolation problem can be defined as construction of a curve say $y(x)$ which passes through a given set of data points (x_i, y_i) for $i = 1, 2, 3...n$ where $x_j > x_i$ with $j > i$. While constructing an approximation curve, one seeks a function best fitted to the given data set. The curve may not pass through the data points. Hermite curbic spline, polynomial interpolation are examples of interpolation functions. B-splines, NURBS are examples of approximation curves.
In the STS motion prediction problem, the trajectory of the joint angles is unknown to us. We may assume the trajectory of joint angle $q_1(t)$ in parametrized form viz.

$$q_1(\boldsymbol{A}, t) = a_0 + a_1 t + a_2 t^2 + a_3 t^3 \tag{2.36}$$

Where $\boldsymbol{A} = (a_0, a_1, a_2, a_3)^T$ is the vector of path parameters. On the other hand we may also parametrize the path using a m segment cubic B-spline curve interpolated at

the endpoints with $m+3$ control points $c_{i1}, c_{i2}...c_{i(m+3)}$.

$$q_1(t) = \sum_{k=1}^{N} B_k(t) c_{1k}, \quad N = 4 \text{ for cubic spline} \tag{2.37}$$

Where $\boldsymbol{C} = (c_{i1}, c_{i2}...c_{i(m+3)})^T$ is the vector of path parameters and B_k are the B-spline basis functions.

In this study, B-spline is chosen because the curve has convex hull property and can be controlled locally [2]. The design variables of the optimization problem clearly are the control points c_{ij} with $i = 1, 2, 3$ and $j = 1, 2...(m+3)$.

wrong figure

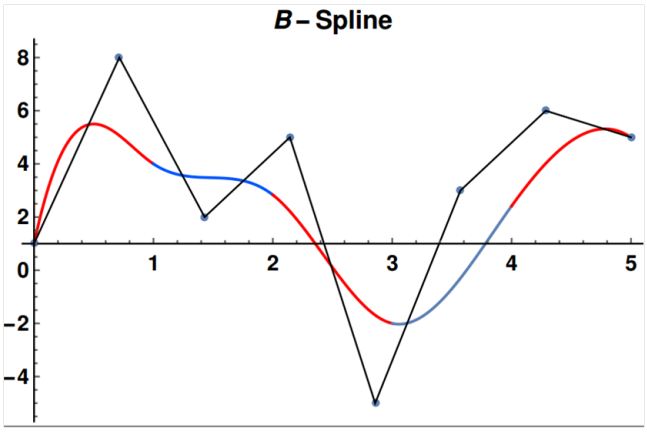

Figure 2.2: A cubic B-spline with interpolated end points

Chapter 3

Simulation of Natural Sit-to-Stand Motion

3.1 Description and Modeling

The natural unaided sit to stand motion is divided into three phases [9].During the first phase, weight is transfered from chair to legs by swinging the upper body. The center of gravity of the body is outside the feet during this phase. Weight of the person is primarily supported by the chair. Second phase consists of transition during which the supporting force by the chair starts falling rapidly. The ZMP [15] lies inside the feet after sit-off takes place even though center of gravity is outside the support polygon. The third phase consists of lifting up the body to standing position.

In this study, STS motion only in the sagittal plane is considered. Sagittal plane is the one which cuts body into left and right. The human is modeled as a three link open chain or in short a 3$\underline{\mathrm{R}}$ planar mechanism pivoted to ground. Though the interface of foot and ground is not a pin joint in real, the assumption remains valid as long as GRF is positive. The joint angle convention chosen is body fixed defined by DH parameters defined in Table 3.1. The DH frames are pictorially illustrated in Fig. 3.1. The green arrows being body fixed $\boldsymbol{z}$ axes and black arrows are body fixed $\boldsymbol{x}$ axes. Link one, two and three correspond to shank, thigh and trunk of the human body respectively. Joint one, two and three correspond to the ankle, knee and hip joints respectively. The link lengths, position of center of mass of links etc. kinematic data and mass, radii of

gyration etc. inertia values were taken from [4]

	α_{i-1}	a_{i-1}	d_i	θ_i
1	0	0	0	θ_1
2	0	l_1	0	θ_2
3	0	l_2	0	θ_3
4	0	l_3	0	0

Table 3.1: DH table for Human modeled as 3R planar mechanism

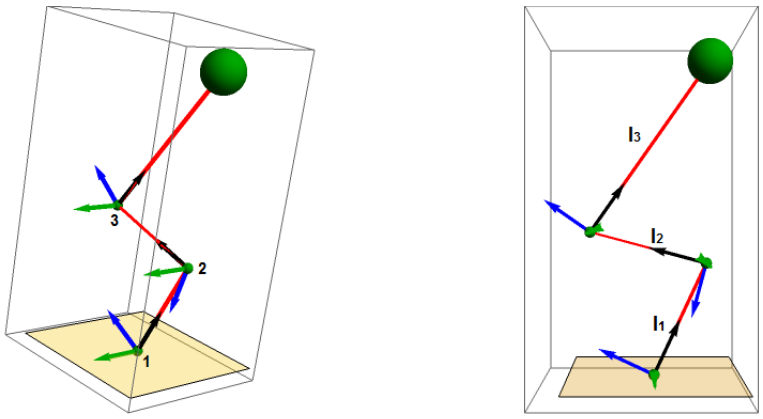

(a) DH frames (b) Link lengths

Figure 3.1: DH frames (Human only)

3.2 Problem formulation

To simulate unaided STS, we wish to obtain a trajectory that minimizes overall effort of the person. The measure of effort can be defined in different ways as discussed in [17]. We use the measure- dynamic effort **DE** and define it as follows-

$$\mathbf{DE} = \int_0^T (\boldsymbol{\tau} \cdot \boldsymbol{\tau}) dt \tag{3.1}$$

Where T is time taken for motion and $\boldsymbol{\tau} = (\tau_1, \tau_2, \tau_3)^T$ is the applied torque at the actuated joints. We wish to minimize **DE**. The trajectory optimization problem is set up as follows

$$\begin{aligned}
\text{Minimize } \mathbf{DE} &= \int_0^T (\boldsymbol{\tau} \cdot \boldsymbol{\tau}) \mathrm{d}t \\
\text{Subject to } \boldsymbol{M}(\boldsymbol{q})\ddot{\boldsymbol{q}} + \boldsymbol{C}(\boldsymbol{q}, \dot{\boldsymbol{q}})\dot{\boldsymbol{q}} + \boldsymbol{G} &= \boldsymbol{\tau} \\
\boldsymbol{q}(t = 0) &= \boldsymbol{q}_{ini} \\
\boldsymbol{q}(t = T) &= \boldsymbol{q}_{end} \\
\boldsymbol{\tau}^{ll} \leq \boldsymbol{\tau} &\leq \boldsymbol{\tau}^{ul} \\
\boldsymbol{q}^{ll} \leq \boldsymbol{q} &\leq \boldsymbol{q}^{ul}
\end{aligned} \tag{3.2}$$

Note that $\boldsymbol{q} = \boldsymbol{q}(t) = (q_1(t), q_2(t), q_3(t))^T$. Where q_1 is angle at ankle, q_2 is angle at knee and q_3 is angle of trunk. The angles are defined uniquely by DH parameters. The solution space $\boldsymbol{q}$ is infinitely large. Therefore, to solve the above optimization problem, we have to discretize the domain. We model $q_i(t)$ as a m segment cubic B-spline curve as specified earlier in equation (2.37). The design variables of the optimization problem clearly are the control points c_{ij} with $i = 1, 2, 3$ and $j = 1, 2...(m + 3)$.

$$q_i(t) = \sum_{k=1}^{N} B_k(t) c_{ik}, \quad N = 4 \text{ for cubic spline} \tag{3.3}$$

$$\dot{q}_i(t) = \sum_{k=1}^{N} \dot{B}_k(t) c_{ik} \tag{3.4}$$

$$\ddot{q}_i(t) = \sum_{k=1}^{N} \ddot{B}_k(t) c_{ik} \tag{3.5}$$

Where B_k are the B-spline basis functions.

3.3 Simulation and Validation of Results

Dynamic modeling of phase one is complicated and requires the support reaction by chair as input to calculate joint torques. The rate at which the supporting force reduces is key input for simulation. The simulations carried out during this study exclude phase one. At the end of phase one, the trunk acquires some angular momentum. Although

the center of gravity may be outside the support polygon at sit-off (see Fig. 3.2), the person does not fall as the ZMP is inside the support polygon of foot. The velocity acquired by the trunk at the end of phase one is taken as input to the simulation from unaided sit to stand experiment.

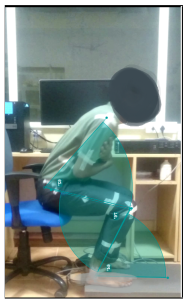

Figure 3.2: Sit-off position captured during STS experiment

3.3.1 Simulation parameters

The initial and final conditions for simulation were chosen by observation from experiments. A typical set of values are shown in Table 3.2 and Fig. 3.3. Time for STS motion was chosen in interval $[1.5, 4]$ seconds, typical value being 2 s. An eight segment B-spline was chosen to provide enough degree of freedom to trajectory. Although no other constraints than upper and lower bounds of design variables were put, the center of gravity remained in the zone of $[0, +20]$ cm from ankle, positive side pointing right in Fig.3.3. 'fmincon' solver in MATLAB ® optimization toolbox was used to solve the set of equations (3.2). The optimized result i.e. the output trajectory depends on the starting point due to the local nature of the solver. Heuristic solvers which calculate global optimum may not be very efficient in this problem as the number of design variables is very high (33 in case of eight segment B-spline). Also they perform poorly in presence of non-linear constraints. So, an exhaustive approach for searching optimum trajectory was taken by choosing more than five set of random starting points for a given boundary condition.

	Ini. Pos $(^0)$	Fin. Pos. $(^0)$	Ini. Velo $(^c/s)$	Fin. Velo. $(^c/s)$
θ_1	63	90	0	0
θ_2	110	0	0	0
θ_3	-113	0	-0.85	0

Table 3.2: Boundary Conditions for unaided STS

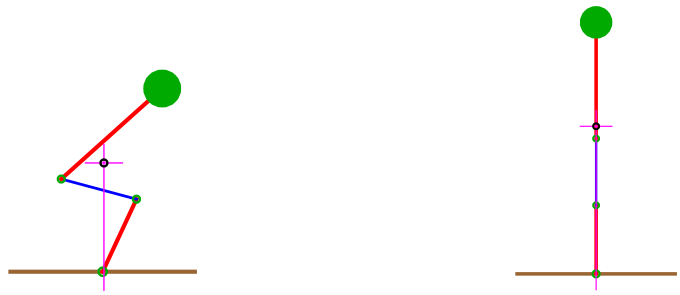

(a) Initial position (b) Final position

Figure 3.3: Boundary conditions for unaided STS

3.3.2 Results and Discussion

Following graphs compare simulated and experimental values of joint angles. Figures 3.4 & 3.5 suggest that the trajectory predicted by simulation has similar characteristics to that of the experimental values.

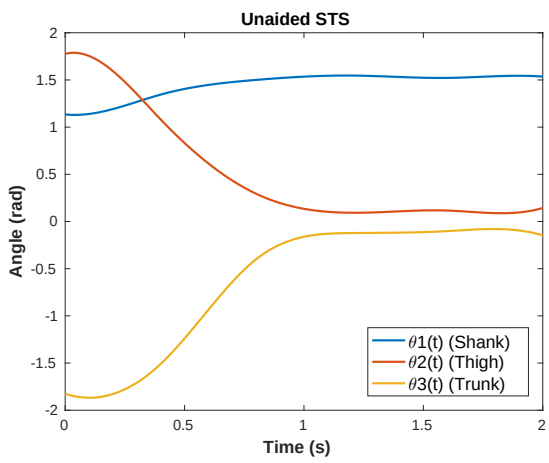

Figure 3.4: Simulated Joint angle variation

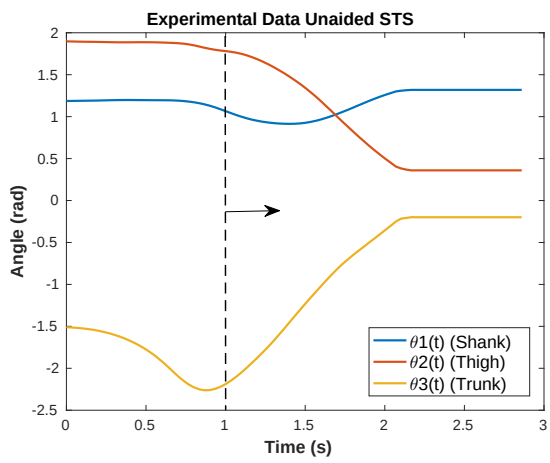

Figure 3.5: Joint angles reconstructed from unaided STS experiment

The ground reaction force (GRF) was calculated for the obtained trajectory. The simulated GRF variation (Fig.3.6) during the course of motion resembles to that of measured value using force plate (Fig 3.7).

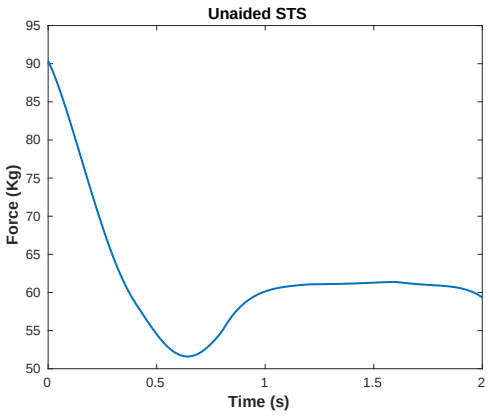

Figure 3.6: Simulated Vertical ground reaction force variation from sit-off to stand up.

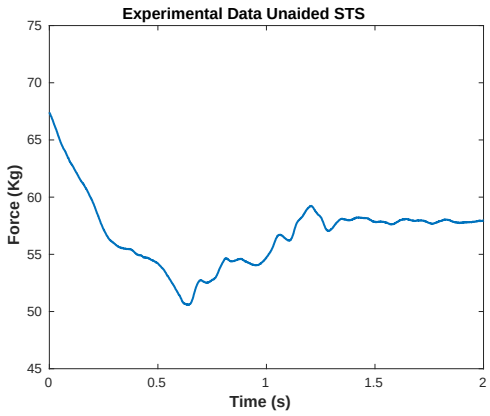

Figure 3.7: Vertical ground reaction force measured by force plates

The STS motion can be visualized with the help of animation snaps (Fig. 3.8) captured at short time intervals.

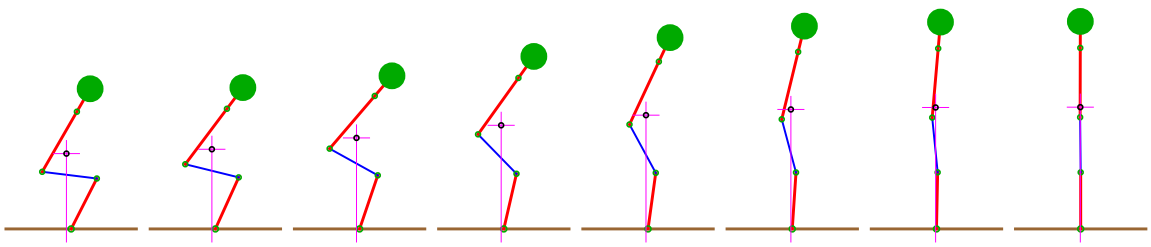

Figure 3.8: Unaided STS Motion visualization

Chapter 4

Simulation of Assisted Sit-to-Stand Motion

4.1 Description and modeling

Sit to stand motion can be aided in several ways. A few ideas are depicted in Fig.4.1 with the green joints as active degrees of freedom. There exist devices that lift the person up completely with no strength required from the side of human. This study takes a minimal aid approach as the device expected to be portable. Proposed sit to stand aid device will provide support to the user at armpits. Human along with the device are modeled as a six link mechanism in sagittal plane. The mechanism thus formed has three degrees of freedom chosen as angle at knee, angle at hip and extension of the device. The assumptions related to modeling of human joints in aided STS are same as those in section 3.1.

The CL STS problem was solved using two sets of joint variables−

$$\boldsymbol{q} = (q_1(t), q_2(t), q_3(t), q_4(t), q_5(t))^T \tag{4.1}$$

$$\boldsymbol{q_b} = (q_{b1}(t), q_{b2}(t), q_{b3}(t), q_{b4}(t), q_{b5}(t))^T \tag{4.2}$$

Where $q_1(t), q_2(t), q_3(t), q_4(t)$ are space fixed angles as depicted in Fig. 4.3 and $\boldsymbol{q_b}$ are body fixed joint variables defined using DH convention as shown in Table 4.1. The DH frames for CL mechanism are shown in Fig. 4.2.

	α_{i-1}	a_{i-1}	d_i	θ_i
1	0	0	0	θ_1
2	0	l_1	0	θ_2
3	0	l_2	0	θ_3
4	0	l_{34}	0	θ_4
5	$-\frac{\pi}{2}$	0	d_5	0

Table 4.1: DH table for Human with device

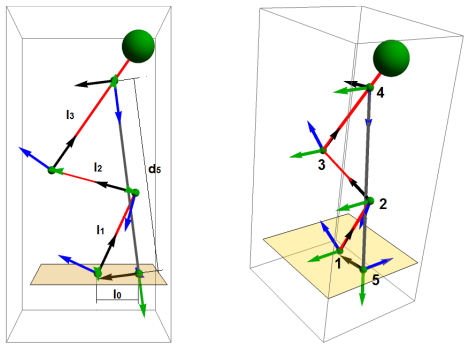

(a) DH frames (b) Link lengths

Figure 4.2: DH frames (Human with device)

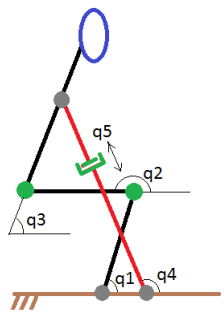

Figure 4.3: Space fixed joint angles

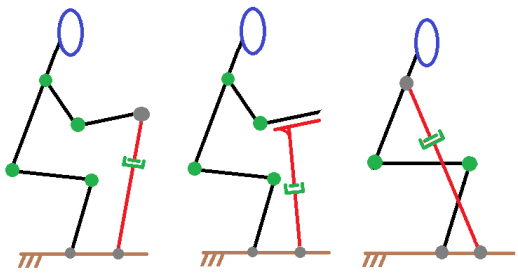

Figure 4.1: Different supporting strategies

4.2 Problem formulation

The trajectory optimization problem for closed loop mechanism is set up as follows

$$
\begin{aligned}
\text{Minimize } \mathbf{DE} &= \int_0^T (\boldsymbol{\tau}_{23} \cdot \boldsymbol{\tau}_{23}) \mathrm{d}t \\
\text{Subject to } & \boldsymbol{M}(\boldsymbol{q})\ddot{\boldsymbol{q}} + \boldsymbol{C}(\boldsymbol{q}, \dot{\boldsymbol{q}})\dot{\boldsymbol{q}} + \boldsymbol{G} = \boldsymbol{\tau} + \underline{\boldsymbol{\tau}^c} \\
& \boldsymbol{q}(t=0) = \boldsymbol{q}_{ini} \\
& \boldsymbol{q}(t=T) = \boldsymbol{q}_{end} \\
& \underline{\boldsymbol{\eta}(\boldsymbol{q}) = 0} \\
& \boldsymbol{\tau}^{ll} \leq \boldsymbol{\tau} \leq \boldsymbol{\tau}^{ul} \\
& \boldsymbol{q}^{ll} \leq \boldsymbol{q} \leq \boldsymbol{q}^{ul}
\end{aligned}
\tag{4.3}
$$

Where $\boldsymbol{\tau}_{23} = (\tau_2, \tau_3)^T$ is torque corresponding to $q_2(t)$ and $q_3(t)$. In closed loop formulation, $\boldsymbol{q} = \boldsymbol{q}(t) = (q_1(t), q_2(t), q_3(t), q_4(t), q_5(t))^T$, complete joint space formulations are used for dynamics. The underlined equations are newly added to set of equations (3.2) used for unaided STS problem. The constrained system can be solved using methods of section 2.2.2. The formulation is done using body fixed set of coordinates (4.2) too. It is awkward to calculate joint reactions in case of Lagrangian formulation. Also, if the coordinates are space fixed, the power $\tau_i \cdot q_i'(t)$ calculated at a degree of freedom is not the power delivered solely by the joint alone. Although the problem is solved with both set of coordinates (4.1) & (4.2), the results corresponding to body fixed coordinates are presented. The validation of the results requires calculation of GRF s which are calculated only using recursive Newton-Euler formulation with body fixed coordinates.

The discretization procedure is similar to equations (3.3). The concern here is that the optimized solution may not evaluate the constraint $\boldsymbol{\eta}(\boldsymbol{q}) = 0$ at every point of time because of the discretization. It the constraint will be valid only at finitely many points equal to those of equality constraints put during optimization. For high accuracy one will have to maple the constraint at large number of discrete points making the task difficult for optimization solver.The issue is resolved if the design variables are reduced to only the active joint variables. The passive variables are solved in terms active joint variables at each step of optimization. However the method may fail if the path hits

singularity at some step of optimization.

The active degrees of freedom are defined earlier in section 4.2. But, the variables for optimization are corresponding to those of $(q_1(t), q_2(t), q_3(t))^T$. As long as valid set of $\boldsymbol{q}, \boldsymbol{q\prime}$ and $\boldsymbol{q\prime\prime}$ are provided, the torques calculated are correct. The calculations for dynamics breakdown at the Type II singularities corresponding to $\boldsymbol{q} = (\boldsymbol{\theta}^T, \boldsymbol{\phi}^T)^T$ where $\boldsymbol{\theta} = (\theta_2, \theta_3, d_5)^T$, $\boldsymbol{\phi} = (\theta_1, \theta_4)^T$ and θ_i and ϕ_i take values q_i or q_{bi} depending upon the method of inverse dynamics. The singularity condition in terms of space fixed angles (Eq. (4.4)) is noted at every step of optimization through a singularity check function during torque calculations.

$$k \cdot \sin(q_1 - q_4) = 0 \tag{4.4}$$

Where k is a non zero constant.

4.3 Simulation and Validation of Results

4.3.1 Simulation parameters

The initial and final conditions for simulation were chosen by observation from experiments. A typical set of values are shown in Table 4.2 and Fig. 4.4. Time for STS motion was chosen in interval $[3, 15]$ seconds, typical value being 5 s. An eight segment B-spline was chosen to provide enough degree of freedom to trajectory. In CL STS simulations, it is crucial to keep check on the pin joint assumption at the ankle as well as the point where assistive device touches ground. Constraints on vertical GRF, horizontal position of center of gravity were put during optimization to ensure the correctness of the simulation.

	Ini. Pos $(^0)$	Fin. Pos. $(^0)$	Ini. Velo $(^c/s)$	Fin. Velo. $(^c/s)$
θ_1	63	88	0	0
θ_2	100	5	0	0
θ_3	-110	-15	0	0

Table 4.2: Boundary Conditions for CL STS

(a) Initial position (b) Final position

Figure 4.4: Boundary Conditions for aided STS

4.3.2 Results and Discussion

The joint angle variations (Fig. 4.5) are observed to be similar to that of natural sit to stand (Fig. 3.4). Formal experiments for aided sit to stand are yet to be conducted but, the GRF variation during aided STS is presented in section 5.2.

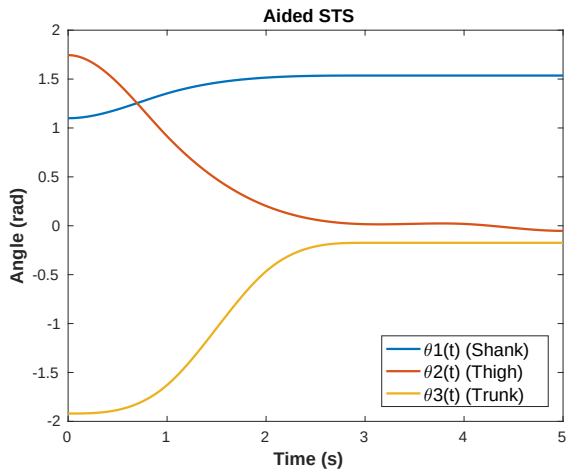

Figure 4.5: Joint angle variation

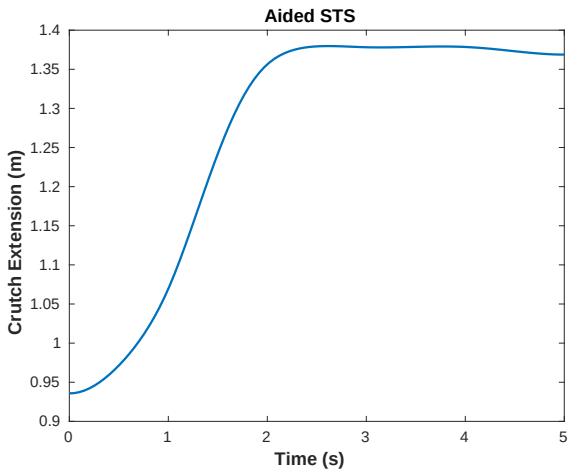

Figure 4.6: Length (d_5) of the device

The maximum knee torque is reduced by almost 40% in case of aided STS motion. The torque variation for OL and CL STS is plotted in Fig. 4.9 and Fig 4.8 respectively. The force corresponding to degree of freedom d_5 is the most sought result. The STS motion is almost complete by 2 s as observed from Fig. 4.6. The force in the device is plotted in Fig. 4.10. The variation of force after 2 s is not of much importance to us, as the device will have a locking provision on complete extension and will work as a rigid link between shoulder and ground. Various simulations show that the horizontal

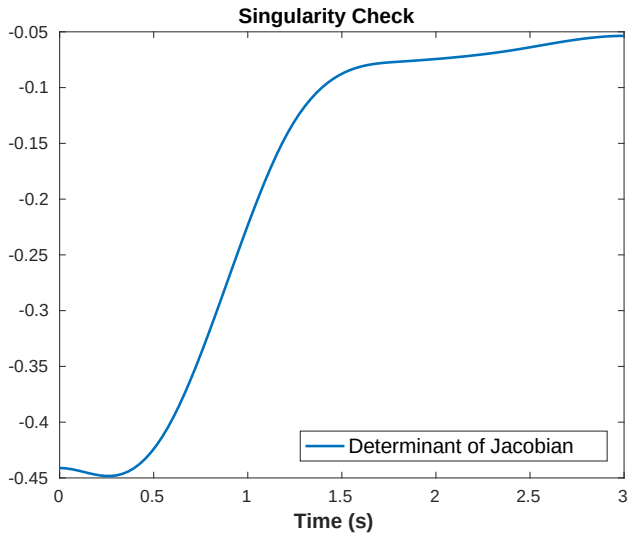

Figure 4.7: LHS of Eq. (4.4) does not vanish at any point in the path

component of GRF does not go above 2 Kg. At a load of say 20 Kg on the device, a coefficient of friction around 0.1 should be good enough to stop the device from slipping. The CL STS motion can be visualized with the help of animation snaps

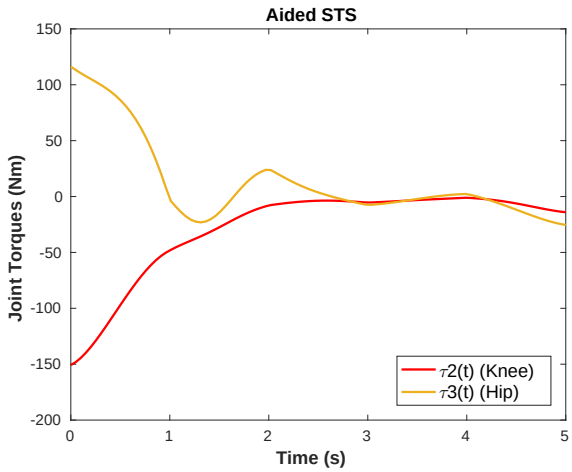

Figure 4.8: Joint torques for CL STS

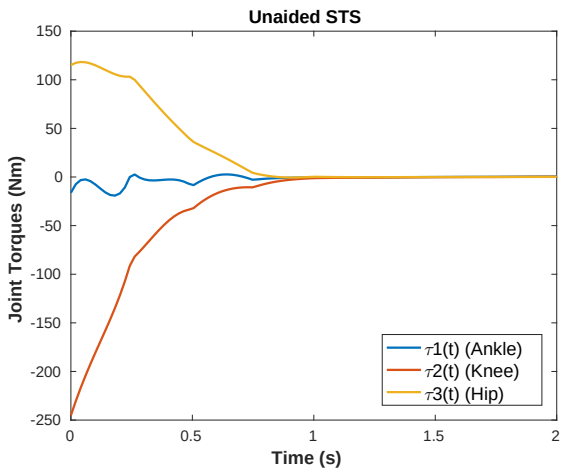

Figure 4.9: Joint torques for OL STS

(Fig. 4.11) captured at short time intervals. The is not enough experimental kinematic data of aided STS to compare with the simulations. However, a experimental data of ground reaction forces in case of both OL and CL STS is available and is compared in next section to find out usefulness of the device.

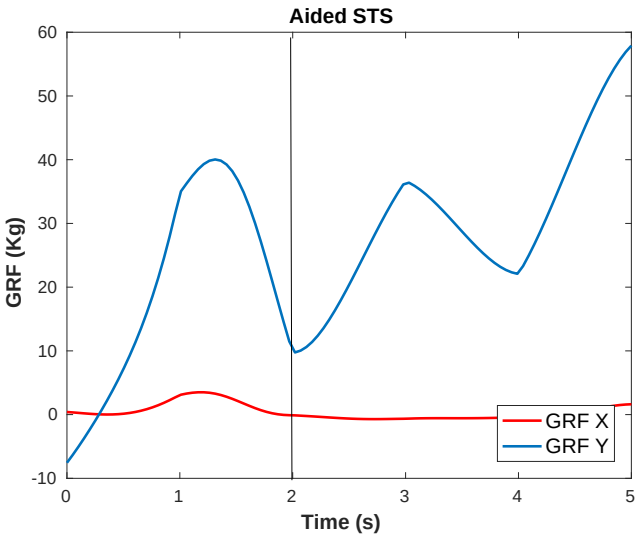

Figure 4.10: Force offered by the assistive device

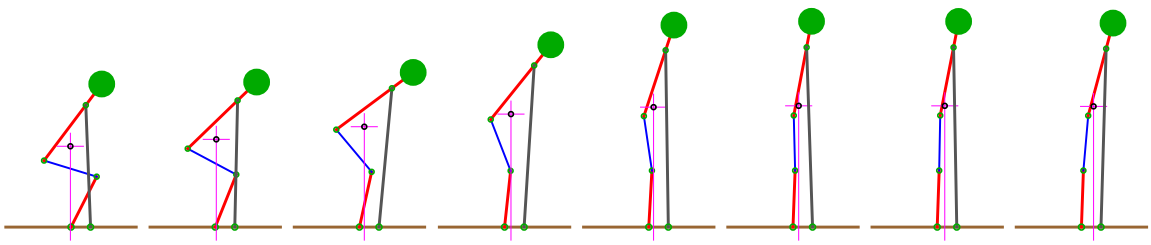

Figure 4.11: Aided STS Motion visualization

Chapter 5

Device Design

5.1 Device Description

The computational model is created in order to get performance parameters of Proposed device looks similar to an axillary crutch. The device assembly consists of two main parts- frame and guide rail. The frame has elbow and forearm support with grip for hands. It slides on a cylindrical hollow guide rail. A tension spring is attached between guide rail and frame. The spring (Fig.5.1c) is in extended position when the device is in compressed state. A locking mechanism is provided to lock the movement of frame at desired position. When unlocked, the spring tries to get back to its original state expanding the device and helping the person to stand up. The device gives back force based on energy recovered in stand to sit motion. A proof of concept prototype of device is manufactured. The device CAD drawings as illustrated in Fig. 5.1.

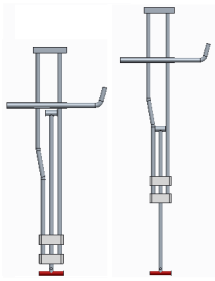

(a) Sitting (left) & standing(right) position

(b) Isomnetric view, CAD model

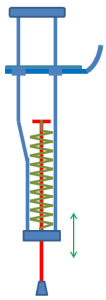

(c) Schematic representation

Figure 5.1: STS aid device

5.2 Comparison of GRF With and Without Device Aid

The center of gravity starts gaining height during phase two and three of unaided STS. The spike in ground reaction (fig.5.2) occurs at the end of phase two (in which weight is transfered from chair to the legs). The data suggests that the device reduces spike in GRF ultimately reducing the joint torques. The device shares more than one third of the body weight. We can observe plateau in fig.5.3 during time 2-13 s followed by a trough and another plateau. The first plateau represents the load on legs at sit-off without the device. As the device starts expanding, it shares the load. After completion of motion at 20 s, the device is put away restoring the load on legs.

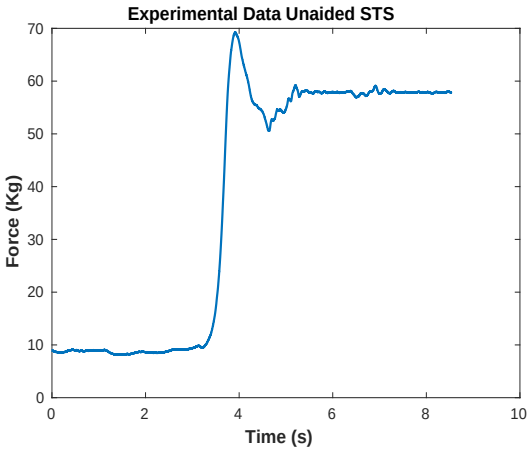

Figure 5.2: Weight supported by legs (GRF) without any aid

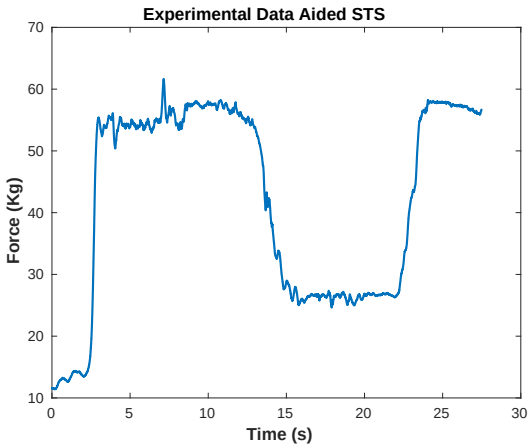

Figure 5.3: Weight supported by legs (GRF) with device in use

Chapter 6

Conclusion and Future Scope

Natural motion of standing up from sitting upright is imitated using optimal control theory. The study of kinematics and dynamics of the motion was constrained to sagittal plane. Optimization of closed loop mechanism has a lot of pitfalls but the problem is resolved by appropriately partitioning the set of active and passive joint variables. The results for OL STS simulation match closely to experimental plots. STS motion simulation with the device aid shows that the knee torque is reduce by 40%. No joint torque is elevated creating unease to the device user.

Following avenues are open for further study

1. Inclusion of constraints on joint torques the resulting motion while minimizing STS effort during aided STS simulations.
2. Experimental study of STS motion with different support strategies.
3. Model human in three dimensions and simulate unaided STS for the same to simulate real life injuries.

Bibliography

[1] Sadiq Mohamed Anwar and Sandipan Bandyopadhyay. Trajectory-tracking control of semi-regular stewart platform manipulator. In *15th National Conference in Machines and Mechanisms*, 2011.

[2] R.H. Bartels, J.C. Beatty, and B.A. Barsky. *An introduction to splines for use in computer graphics and geometric modeling.* Morgan Kaufmann Series in Computer Graph Series. M. Kaufmann Publishers, 1987.

[3] J.J. Craig. *Introduction to Robotics: Mechanics and Control.* Addison-Wesley series in electrical and computer engineering: Control engineering. Addison-Wesley, 1989.

[4] Paolo De Leva. Adjustments to zatsiorsky-seluyanov's segment inertia parameters. *Journal of biomechanics*, 29(9):1223–1230, 1996.

[5] J DENAVIT. A kinematic notation for lower-pair mechanisms based on matrices. *Trans. of the ASME. Journal of Applied Mechanics*, 22:215–221, 1955.

[6] Janzen Lo, Gang Huang, and Dimitris Metaxas. Human Motion Planning Based on Recursive Dynamics and Optimal Control Techniques. *Multibody System Dynamics*, 8:433–458, 2002.

[7] Margaret K Y Mak, Oron Levin, Joseph Mizrahi, and Christina W Y Hui-Chan. Joint torques during sit-to-stand in healthy subjects and people with Parkinson's disease. *Clinical Biomechanics*, 2003.

[8] L. Meirovitch. *Methods of analytical dynamics.* Advanced engineering series. McGraw-Hill, 1970.

[9] Pamela J. Millington, Barbara M. Myklebust, and Georgia M. Shambes. Biomechanical analysis of the sit-to-stand motion in elderly persons. *Archives of Physical Medicine and Rehabilitation*, 73(7):609–617, July 1992.

[10] Richard M Murray, Zexiang Li, S Shankar Sastry, and S Shankara Sastry. *A mathematical introduction to robotic manipulation*. CRC press, 1994.

[11] Yoshihiko Nakamura and Modjtaba Ghodoussi. Dynamics Computation of Closed-Link Robot Mechanisms with Nonredundant and Redundant Actuators. *IEEE Transactions on Robotics and Automation*, 5(3):294–302, 1989.

[12] Chaman Nasa and Sandipan Bandyopadhyay. Trajectory-tracking control of a planar 3-rrr parallel manipulator with singularity avoidance. In *13th World Congress in Mechanism and Machine Science*, pages 19–25, 2011.

[13] Burak Ozsoy. *Three dimensional Sit to Stand Motion Prediction*. PhD thesis, 2014.

[14] S. Rakshit and S. Akella. A trajectory optimization formulation for assistive robotic devices. In *2016 IEEE International Conference on Robotics and Automation (ICRA)*, pages 2068–2074, May 2016.

[15] Miomir Vukobratović and Branislav Borovac. Zero-moment point-thirty five years of its life. *International Journal of Humanoid Robotics*, 1(01):157–173, 2004.

[16] Yujiang Xiang, Jasbir S. Arora, and Karim Abdel-Malek. Optimization-based motion prediction of mechanical systems: sensitivity analysis. *Structural and Multidisciplinary Optimization*, 37(6):595, 2008.

[17] Yujiang Xiang, Jasbir S Arora, and Karim Abdel-Malek. Physics-based modeling and simulation of human walking: a review of optimization-based and other approaches. *Struct Multidisc Optim*, 42:1–23, 2010.